



Communication

Synthesis, Molecular Docking and Antiplasmodial Activities of New Tetrahydro- β -Carbolines

Anna Jaromin ^{1,*}, Beata Gryzlo ², Marek Jamrozik ², Silvia Parapini ³, Nicoletta Basilico ⁴, Marek Cegla ², Donatella Taramelli ⁵ and Agnieszka Zagórska ^{2,*}

¹ Department of Lipids and Liposomes, Faculty of Biotechnology, University of Wrocław, Joliot-Curie 14a, 50-383 Wrocław, Poland

² Faculty of Pharmacy, Jagiellonian University Medical College, 30-688 Kraków, Poland; beata.gryzlo@uj.edu.pl (B.G.); marek.jamrozik@doctoral.uj.edu.pl (M.J.); marek.cegla@uj.edu.pl (M.C.)

³ Dipartimento di Scienze Biomediche per la Salute, Università degli Studi di Milano, 20133 Milan, Italy; silvia.parapini@unimi.it

⁴ Dipartimento di Scienze Biomediche, Chirurgiche e Odontoiatriche, Università degli Studi di Milano, 20133 Milan, Italy; nicoletta.basilico@unimi.it

⁵ Dipartimento di Scienze Farmacologiche e Biomolecolari, Università degli Studi di Milano, 20133 Milan, Italy; donatella.taramelli@unimi.it

* Correspondence: anna.jaromin@uwr.edu.pl (A.J.); agnieszka.zagorska@uj.edu.pl (A.Z.)

Citation: Jaromin, A.; Gryzlo, B.; Jamrozik, M.; Parapini, S.; Basilico, N.; Cegla, M.; Taramelli, D.; Zagórska, A. Synthesis, Molecular Docking and Antiplasmodial Activities of New Tetrahydro- β -Carbolines. *Int. J. Mol. Sci.* **2021**, *22*, 13569. <https://doi.org/10.3390/ijms222413569>

Academic Editors: Geoffrey Brown, Andrzej Kutner and Enikő Kallay

Received: 8 November 2021

Accepted: 13 December 2021

Published: 17 December 2021

Publisher's Note: MDPI stays neutral with regard to jurisdictional claims in published maps and institutional affiliations.



Copyright: © 2021 by the authors. Licensee MDPI, Basel, Switzerland. This article is an open access article distributed under the terms and conditions of the Creative Commons Attribution (CC BY) license (<http://creativecommons.org/licenses/by/4.0/>).

Abstract: Malaria is still one of the most dangerous infectious diseases and the emergence of drug resistant parasites only worsens the situation. A series of new tetrahydro- β -carbolines were designed, synthesized by the Pictet–Spengler reaction, and characterized. Further, the compounds were screened for their in vitro antiplasmodial activity against chloroquine-sensitive (D10) and chloroquine-resistant (W2) strains of *Plasmodium falciparum*. Moreover, molecular modeling studies were performed to assess the potential action of the designed molecules and toxicity assays were conducted on the human microvascular endothelial (HMEC-1) cell line and human red blood cells. Our studies identified *N*-(3,3-dimethylbutyl)-1-octyl-2,3,4,9-tetrahydro-1H-pyrido[3,4-*b*] indole-3-carboxamide (**7**) (a mixture of diastereomers) as the most promising compound endowed with the highest antiplasmodial activity, highest selectivity, and lack of cytotoxicity. In silico simulations carried out for (1*S*,3*R*)-**7** provided useful insights into its possible interactions with enzymes essential for parasite metabolism. Further studies are underway to develop the optimal nanosized lipid-based delivery system for this compound and to determine its precise mechanism of action.

Keywords: tetrahydro- β -carbolines; *Plasmodium falciparum* (*P. falciparum*); antimalarial; antiparasitic agents; cytotoxicity; hemolysis; molecular docking

1. Introduction

Malaria is an infectious disease caused by the protozoan parasite of the genus *Plasmodium*, with *Plasmodium falciparum* and *Plasmodium vivax* being predominantly responsible for mortality and morbidity. In 2019, the global tally of malaria cases was 229 million, an annual estimate that has remained virtually unchanged over the last 4 years [1]. Despite the Covid-19 pandemic, an analysis of malaria prevention showed that the 2020 campaigns to control and eradicate malaria were realized as planned. Lastly, in October of 2021, the WHO has recommended Mosquirix, the RTS,S/AS01 malaria vaccine, for the prevention of *P. falciparum* malaria in children living in regions with moderate to high transmission [2]. However, disruptions to continued access to effective antimalarial treatment could lead to considerable loss of life [3].

First-line malaria treatments include several artemisinin-based combination therapies (ACTs), such as artemether-lumefantrine (AL), artesunate-amodiaquine (AS-AQ), artesunate-sulfadoxine-pyrimethamine (AS+SP), artesunate-mefloquine (AS-MQ),

and dihydroartemisinin-piperaquine (DHA-PPQ). The malaria problem is evolving, dynamic, and diverse, mainly due to the intrinsic ability of *P. falciparum* to acquire resistance against drugs. *P. falciparum* has developed resistance to nearly all currently available antimalarial drugs, such as sulfadoxine/pyrimethamine, mefloquine, halofantrine, and quinine [4]. The observed decrease in the effectiveness of artemisinin is correlated with mutation in the *P. falciparum* Kelch13 gene [5]. In addition, there is resistance against artemisinin partner drugs, such as mefloquine and piperaquine [6,7]. Thus, there is an urgent need to find a replacement for artemisinin or novel artemisinin partner-drugs active against known-resistant strains. Currently, all new molecules are tested against a wide variety of resistant laboratory strains of *P. falciparum*, and activity in these assays is a key requirement for further evaluation.

The 1,2,3,4-Tetrahydro- β -carboline (9H-1,2,3,4-tetrahydropyrido(3,4-b)indole, TH β C) core (Figure 1) is a privileged structure found in many antimalarial drug candidates and represents an important scaffold for the discovery of novel potent antimalarials. Among the TH β C, C1–C3 substituted derivatives were reported as having potent antimalarial activity [8]. Cipargamin (KAE609, NITD609) (Figure 1) is a novel spiroindolone-class drug for the treatment of malaria. The compound displayed low nanomolar 50% inhibitory concentration (IC₅₀) values (range 0.5–1.4 nM), with no evidence of diminished potency against drug-resistant strains. Cipargamin acts on the P-type Na⁺ ATPase (PfATP4) of *P. falciparum*, disrupting its Na⁺ homeostasis. This mechanism is distinct from that of existing antimalarial drugs. Currently, cipargamin is undergoing a phase 2 clinical trial [9].

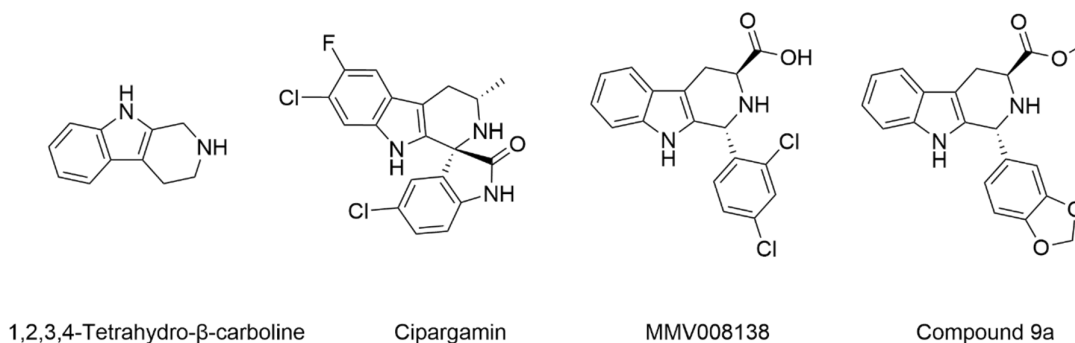


Figure 1. Examples of TH β C derivatives with potent antimalarial activity.

Similarly, compound MMV008138 (Figure 1) exhibits potent antimalarial activity and inhibits the growth of the *P. falciparum* Dd2 strain with an IC₅₀ of 250 nM [10]. Gorki et al. explored the antimalarial activity of a β -carboline derivative, compound **9a** (Figure 1), against *P. falciparum*. Compound **9a** inhibited both the 3D7 and RKL-9 strains of *P. falciparum* with an IC₅₀ < 2.86 μ M, respectively, was nontoxic to normal dermal fibroblasts, and its selectivity index was >10 against both strains [11]. Further, Gellis et al. reported on a series of 1-phenyl-substituted- β -carboline derivatives with significant antimalarial activity (0.7 < IC₅₀ < 1.7 mM) against the W2 multidrug-resistant strain of *P. falciparum* [12].

Considering these promising antimalarial activities of various TH β C derivatives, we designed and synthesized a new series of compounds with aromatic and/or aliphatic side chains in the 1-position and an amide bond in the 3-position of TH β C (Figure 2). The known TH β C derivatives active against the drug-resistant *P. falciparum* contain mostly bulky aromatic or heteroaromatic substituents (such as piridyl, piperonyl, thiophene, or di-chlorophenyl moieties) at the C1 position and small methyl esters at the C3 position. Consequently, we decided to change the physicochemical properties of the substituents at the C1 and C3 positions, namely, from bulky to small at the C1 position and from small to bulky at the C3 position. The target compounds in the further biological investigations

that were conducted, were used as undetermined mixtures of enantiomers and as pure diastereomers or as a mixture of diastereomers.

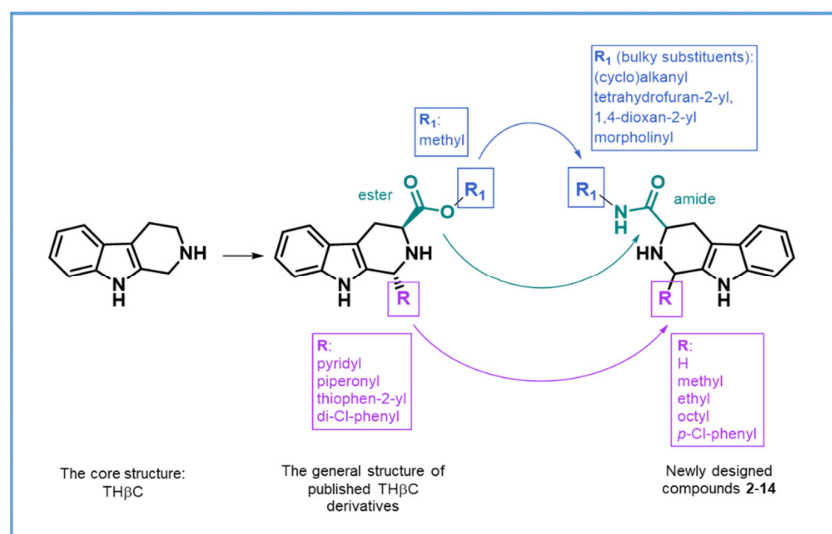


Figure 2. Modification of THβC and general structure of the new compounds (2–14).

The synthesized compounds were evaluated for *in vitro* activity against D10 (CQ-sensitive) and W2 (CQ-resistant) strains of *P. falciparum*. Subsequently, the cytotoxic activity on human microvascular endothelial cells and hemolytic effects on human erythrocytes were also investigated, to obtain more information concerning their safety against mammalian cells. Moreover, compounds 2–14 were also characterized by their physicochemical parameters (Log D). Next, we focused on the probable mechanism of action of the most active compound. Thus, molecular modeling studies were performed to assess the potential binding modes of one enantiomer of compound 7 (that is (1*S*,3*R*)-7) with a series of different enzymes essential for parasite metabolism. Phosphoethanolamine methyltransferase (PMT) plays a critical function in parasite development and differentiation but is absent in mammals. PMT catalyzes the synthesis of phosphatidylcholine—the major phospholipid constituent of the membranes of parasites during the sexual and asexual stages of *Plasmodium* [13]. Lactate dehydrogenase (LDH) is synthesized by parasites in the blood-stage of malaria as the terminal enzyme in the glycolytic pathway of *Plasmodium* [14]. Cytosolic malate dehydrogenase (MDH) converts malate to oxaloacetate and, as a result, generates NADH or NADPH, two reducing equivalents to the respiratory chain of *Plasmodium* [15]. Falcipain-2 (FP2) and falcipain-3 (FP3) are critical hemoglobins of *P. falciparum*, which catalyze the degradation of hemoglobin into hemozoin [16].

For this, five different enzymes of *P. falciparum* were selected for docking studies with the view of investigating a possible multitargeting mode of action. Such a strategy would constitute a promising solution to *P. falciparum* drug resistance. To our knowledge, this is the first study describing the syntheses of this type of tetrahydro-β-carboline series as well as their antiplasmodial activities and the *in silico* approach used to study their probable mechanisms of action on this parasite.

2. Results and Discussion

2.1. Chemistry

The synthesis of the designed THβC derivatives (2–14) commenced with the Pictet–Spengler reaction of racemic tryptophan and an appropriate aldehyde in the presence of sulfuric acid (H₂SO₄) in water (Figure 3) [17]. The resultant 1-substituted-tetrahydro-β-carboline-3-carboxylic acids (1a–e) were further reacted with diverse amines in the

presence of 4-dimethylaminopyridine (DMAP), 1-ethyl-3-(3-dimethylaminopropyl) carbodiimide (EDC), 1-hydroxybenzotriazole (HOBt), and pyridine. The final compounds were purified by crystallization from hexane or by column chromatography. The structures and purity of the newly synthesized compounds were characterized by ^1H NMR, ^{13}C NMR spectroscopy, and UPLC/MS spectrometry. Compounds were isolated as an undetermined mixture of enantiomers (3*RS*-2, 1*RS*,3*SR* for 8–11 and 14), pure diastereomers (1*RS*,3*RS*-13, 1*RS*,3*SR*-13) or as a mixture of diastereomers (1, 3–7, 12) with various diastereoselectivity (ds) (Section Materials and Methods, Section 3.1).

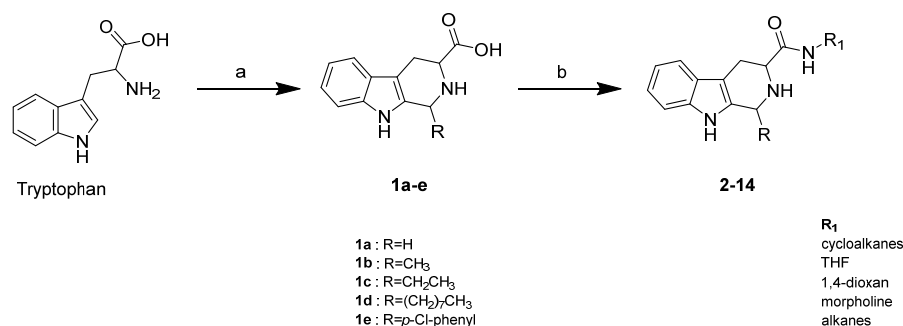


Figure 3. Synthesis of compounds 2–14. Reagents and conditions: (a) RCHO, H₂SO₄, H₂O, reflux or rt, 20 h; (b) amine, DMAP, EDC, HOBt, pyridine, DCM, reflux, 24 h.

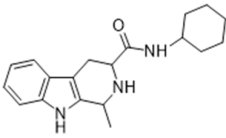
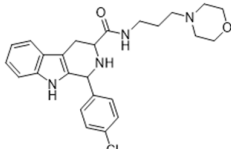
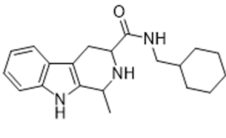
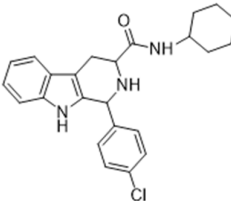
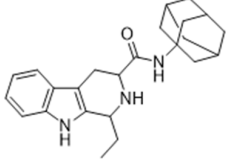
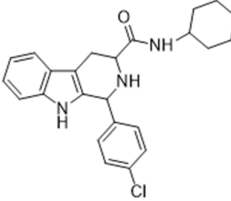
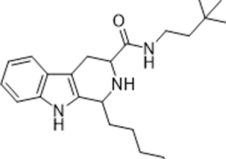
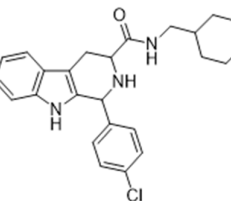
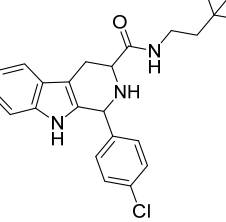
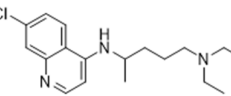
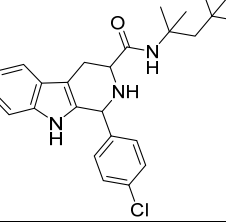
The applied synthetic methods facilitated the synthesis of intermediates (1a–e), and compounds (2–14), with yields of 15–74% and the purity of the final compounds above 95%.

2.2. Log D Calculation

Compounds 2–14 are partially ionized; thus, the distribution coefficients D (Log D) were calculated at fixed pH. The chosen pH (7.4, 7.2, and 5.5) represent the physiological conditions found in the blood, human erythrocyte cytoplasm, and *P. falciparum* food vacuoles. The data in Table 1 show that, for Log D at pH 7.4, the compounds fall in the range 1.73–5.65, and in the range of 1.59–5.53 at pH 7.2, whereas at pH 5.5, the compounds were in the range of 0.05–3.93. Only compound 3 displayed a gradient of Log D similar to CQ, however, the values of Log D for compound 3 were almost twice as large as those for CQ itself.

Table 1. Prediction of Log D for compounds 2–14 and CQ.

Comp	Structure	Log D			Comp	Structure	Log D		
		pH 7.4	pH 7.2	pH 5.5			pH 7.4	pH 7.2	pH 5.5
2		2.53	2.40	0.87	10		3.39	3.34	2.12
3		1.73	1.59	0.05	11		2.77	2.71	1.50

4		2.47	2.33	0.80	12		2.69	2.53	0.05
5		2.79	2.65	1.11	1RS,3RS-13		4.47	4.72	3.50
6		3.18	3.03	1.47	1RS,3SR-13		4.47	4.72	3.50
7		5.65	5.49	3.93	14		5.09	5.03	3.82
8		4.88	4.83	3.61	CQ		0.88	0.64	0.76
9		5.58	5.53	4.31					

2.3. Antiplasmodial Activities

Next, the screening of antiplasmodial activities in in vitro parasite cultures was performed using standard procedures. For this purpose, we tested the susceptibility of two strains of *P. falciparum* differing in resistance to CQ, namely D10 (chloroquine-sensitive) and W2 (chloroquine-resistant). The inhibitory effect on the growth of these strains, expressed as IC₅₀ values, is presented in Table 2. The synthesized derivatives have IC₅₀ values in the range of 4.00 ± 0.53–35.36 ± 4.86 μM. The highest antiplasmodial activity among the tested series was shown by compound 7, which is also characterized by one of the highest Log D values in the series of compounds. Moreover, many compounds have a similar magnitude of inhibitory activity against the two *P. falciparum* strains, as reported for other tetrahydro-β-carboline derivatives by Eagon et al. [18]. The important fact is also that, except for compound 6, the determined values of IC₅₀ are lower for the CQ-resistant strain in comparison to the CQ-sensitive strain, reflected in their RI (resistance index)

values. This could suggest superior sensitivity of the designed compounds towards the CQ-resistant parasite strain. The obtained results are very encouraging, especially since malaria control is threatened by the emergence of drug resistance to the artemisinin derivatives [19]. The data also indicate a different relationship between chemical structure and antiparasmodial activity that is not directly related to Log D values and the types of chemical substituents.

Table 2. The antiparasmodial activity of compounds (2–14) against the D10 (CQ-sensitive) and W2 (CQ-resistant) strains of *P. falciparum* and relevant RI.

Compound	<i>P. falciparum</i> IC ₅₀ (μM)		RI ^a
	D10	W2	
2	21.87 ± 5.82	10.12 ± 2.14	0.46
3	13.17 ± 2.85	9.60 ± 0.78	0.73
4	21.38 ± 4.70	20.10 ± 2.79	0.94
5	33.47 ± 7.58	16.19 ± 4.11	0.48
6	9.73 ± 0.96	11.36 ± 0.82	1.17
7	4.45 ± 0.83	4.00 ± 0.53	0.90
8	10.48 ± 1.53	7.80 ± 1.54	0.74
9	8.41 ± 1.20	6.41 ± 1.05	0.76
10	29.36 ± 7.88	20.54 ± 2.20	0.70
11	35.36 ± 4.86	29.07 ± 4.05	0.82
12	11.45 ± 0.34	6.15 ± 0.46	0.54
1RS,3RS-13	16.05 ± 3.36	13.46 ± 1.99	0.84
1RS,3SR-13	12.53 ± 0.71	9.13 ± 0.83	0.73
14	– ^b	– ^b	–
CQ	0.017 ± 0.006	0.27 ± 0.07	15.88

^a RI = IC₅₀ CQ resistant *P. falciparum* strain/IC₅₀ CQ sensitive *P. falciparum* strain; ^b IC₅₀ > 47.40 μM;

2.4. Biocompatibility Studies

Results from the preliminary antiparasmodial activity screening highlighted the necessity for the evaluation of the safety of these agents to human cells. Hence, we chose two model cell systems: the human microvascular endothelial (HMEC-1) cell line and human erythrocytes, to obtain greater insights into their cell toxicity potential. In these studies, we focused only on derivatives that had exhibited the highest antiparasmodial activities, namely 3, 6, 7, 8, 9, 12, 1RS,3RS-13, and 1RS,3SR-13. The results concerning their cytotoxic effects on HMEC-1 cells as well as their calculated selectivity index (SI), namely the ratio between the IC₅₀ values on the endothelial cells and that on the *Plasmodium* strains, are summarized in Table 3. Based on the analysis of the obtained results, it can be concluded that the determined IC₅₀ values fall within a fairly wide range from 17.95 ± 9.46 to 157.18 ± 42.50 μM, even though they all have their IC₅₀ in the range of low micromolar concentrations against both strains of *Plasmodium*. A similar phenomenon has already been described for methoxy-thiazinoquinones by Imperatore et al. [20]. Interestingly, the most active compound against the parasite (7) is also safe to HMEC-1 cells and is highly selective, also exhibiting the highest SI value of the whole compound series.

Table 3. Cytotoxicity of compounds **3**, **6**, **7**, **8**, **9**, **12**, **1RS,3RS-13**, **1RS,3SR-13**, and **CQ** on the HMEC-1 cell line and relevant selectivity indexes (SI).

Compound	IC ₅₀ (μM)	SI ^a	
		D10	W2
3	157.18 ± 42.50	11.93	16.37
6	21.09 ± 8.82	2.17	1.86
7	72.02 ± 22.40	16.18	18.00
8	17.95 ± 9.46	1.71	2.30
9	18.93 ± 10.16	2.25	2.95
12	102.07 ± 14.83	8.91	16.60
1RS,3RS-13	53.78 ± 21.89	3.35	4.00
1RS,3SR-13	- ^b	-	-
CQ	>38 ^c	-	-

^a SI = IC₅₀ HMEC-1/IC₅₀ *P. falciparum* strain; ^b IC₅₀ > 122.57 μM; ^c data from [21].

We also sought to investigate the hemolytic potential of the synthesized compounds. For this experiment, we selected three compounds, namely **3**, **7**, and **12**, which exhibited the highest selectivity. We incubated these compounds at a concentration of 10 μM, with human erythrocytes, and then, by measuring the released hemoglobin, we assessed their potential harmful effects on these cells. The measured level of hemolysis was less than 5% for all agents, which proves that the compounds are not hemolytic. It is worth emphasizing at this point that this type of test is extremely important to confirm that the observed inhibitory activity against *Plasmodium* is a result of a compound acting directly upon it and not as a result of red blood cell lysis. Taking into account the fact that the tested concentration of **7** in this test was, respectively, 2.2 and 2.5 times higher than the IC₅₀ determined for the *Plasmodium* strains, we can conclude that the observed effect on the parasite is not due to activity on erythrocytes. In conclusion, compound **7** is, therefore, biocompatible, since no hemolytic effects were detected in the mammalian cells tested.

2.5. Molecular Modeling

Molecular modeling studies were performed to evaluate the possible mechanism of action of the one enantiomer of compound **7** namely (1*S*,3*R*)-3-[(3,3-dimethylbutyl)carbamoyl]-1-octyl-1*H*,2*H*,3*H*,4*H*,9*H*-pyrido[3,4-*b*]indol-2-ium (*trans*); (compound (1*S*,3*R*)-**7**). The LigPrep tool and MarvinSketch software indicated that, at pH 7.4, 73% of compound (1*S*,3*R*)-**7** molecules exist in the form where the 1,2,3,6-tetrahydropyridine ring has a protonated amine group, whereas 27% of molecules remain uncharged. Faced with such a clear disproportion, we assumed that the protonated form is responsible for most of the physiological effect and, consequently, only this form was used in the docking simulations. Compound (1*S*,3*R*)-**7** was docked to the following series of enzymes essential for the functioning of *P. falciparum*: phosphoethanolamine methyltransferase (PMT), falcipain-2 (FP2), falcipain-3 (FP3), lactate dehydrogenase (LDH), and malate dehydrogenase (MDH). Moreover, compound (1*S*,3*R*)-**7** formed molecular interactions with the amino acid residues of these enzymes, as observed in the originally co-crystallized ligands.

In the complex of compound (1*S*,3*R*)-**7** and PMT that was obtained by IFD simulations (Figure 4A), a π -cation interaction between Tyr27 of PMT and the protonated amine group of tetrahydropyridine, as well as hydrogen-bonding between the side chain of Lys247 of PMT and the oxygen in the amide moiety of compound (1*S*,3*R*)-**7** were observed. Moreover, both mentioned amino acid residues participated in forming interactions with phosphocholine in the PMT crystal. In addition, a π - π interaction was observed between Tyr19 of PMT and the aromatic benzene ring from the β -carboline moiety. This additional interaction was not observed in the PMT crystal structure.

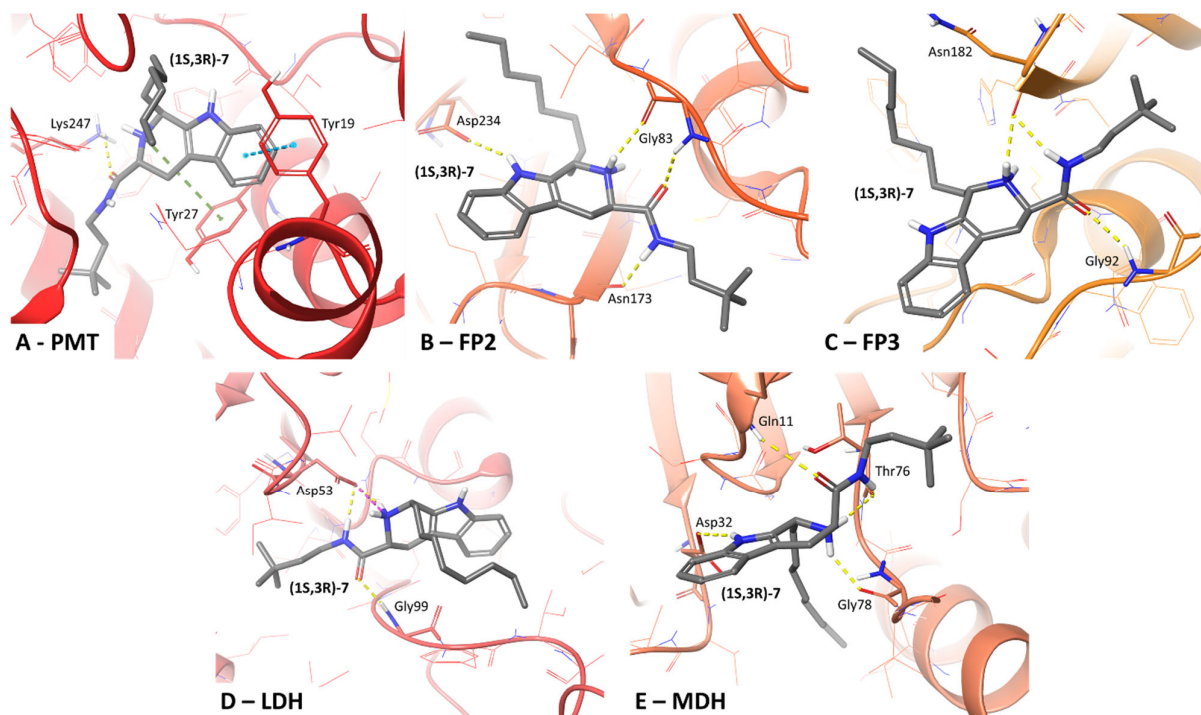


Figure 4. Molecular interactions formed between compound (1S,3R)-7 and selected molecular targets phosphoethanolamine methyltransferase (PMT) (A); falcipain-2 (FP2) (B); falcipain-3 (FP3) (C); lactate dehydrogenase (LDH) (D); and malate dehydrogenase (MDH) (E). Amino acid residues within 4 Å from the ligand are displayed as thin sticks; amino acid residues engaged in ligand binding by ionic bond (dotted pink lines), H-bond (dotted yellow lines), π -cation interaction (dotted green lines), and π - π interaction (dotted blue lines) are displayed as bold sticks.

The obtained complex of compound (1S,3R)-7 and falcipain-2 (Figure 4B) formed H-bonds between the main chain of Gly83 in PMT and the protonated amine group of tetrahydropyridine and the oxygen in the amide moiety of compound (1S,3R)-7. A hydrogen-bond was also observed between the main chain of Asn173 of PMT and the hydrogen on the amide grouping in compound (1S,3R)-7. All the amino acid residues discussed previously formed interactions with epoxysuccinate in the FP2 crystal. However, the H-bond between the side chain of Asp234 and the amine group of the center ring of β -carboline was not observed in the FP3 crystal structure.

The complex of FP3 (Figure 4C) and compound (1S,3R)-7 formed H-bonds between the main chain of Asn182 and the protonated amine group of tetrahydropyridine, as well as with hydrogen from the amide of compound (1S,3R)-7. In addition, a hydrogen bond between the main chain of Gly92 of FP3 and the amide's oxygen of compound (1S,3R)-7 was observed. It is noteworthy that all the mentioned amino acid residues participated in interactions with leupeptin in the FP3 crystal.

An ionic bond (salt bridge) was observed between the side chain of Asp53 in LDH and the protonated amine group of tetrahydropyridine of compound (1S,3R)-7, as well as a hydrogen bond between the side chain of Asp53 and the hydrogen of the amide group of compounds (1S,3R)-7, and an additional H-bond identified between the main chain of Gly99 and the oxygen of the amide group of compounds (1S,3R)-7 (Figure 4D). All the mentioned amino acid residues participated in forming interactions with NADH in the LDH crystal.

Compound (1S,3R)-7 (Figure 4E) formed a hydrogen bond between the main chain of MDH's Gly78 and the protonated amine group of tetrahydropyridine, along with an H-bond between the main chain of Thr76 and the protonated amine group of tetrahydropyridine and the hydrogen of the amide moiety of compound (1S,3R)-7. A further H-bond exists between the main chain of Gln11 and the oxygen on the amide

moiety of compound (1*S*,3*R*)-7, and an H-bond between the side chain of Asp32 and the amine group of the center ring of β -carboline of compound (1*S*,3*R*)-7. Among the mentioned amino-acid interactions, only Thr76 was not involved in forming interactions with NAD in the 6R8G crystal.

Results from IFD revealed that each H-bond donor/acceptor fragment present in compound (1*S*,3*R*)-7, such as the amine group of the center ring of β -carboline, the protonated amine group on tetrahydropyridine, and the oxygen, nitrogen, and hydrogen atoms of the amide moiety of compound (1*S*,3*R*)-7, were involved in forming an interaction with at least one amino-acid target in the group of enzymes investigated. Moreover, the aliphatic chains of compound (1*S*,3*R*)-7 additionally stabilized the position of the entire molecule within the enzymes. Observations from *in silico* simulations highlight that compound (1*S*,3*R*)-7 has structural features enabling it to interact with five described molecular targets within sites occupied originally by other ligands (products/inhibitors/cofactors). The results are a good starting point for further *in vitro* evaluation of compound (1*S*,3*R*)-7.

3. Materials and Methods

3.1. General Remarks

Commercially available reagents were purchased from Merck-Sigma-Aldrich (Poznań, Poland), Acros Organics (Thermo Fisher Scientific, Waltham, MA, USA), or ChemPur (Piekary Śląskie, Poland) and were used without further purification. Purification of chemical compounds by column chromatography was carried out using silica gel mesh: 0.063–0.200 μ m (Sigma-Aldrich; Poznań, Poland) as a stationary phase. The reactions were monitored by thin-layer chromatography on aluminum sheets precoated with silica gel 60 F₂₅₄ (Merck; Darmstadt, Germany). Compounds were visualized with UV light (254 nm). In addition, chromatograms were stained in a 0.5% solution of ninhydrin in *n*-propanol or a solution of 5% (NH₄)₆Mo₇O₂₄ and 0.2% Ce(SO₄)₂ in 5% H₂SO₄. The retardation factor *R_f* was defined using the following solvent systems: S₁ (DCM/methanol/acetic acid, 8:2:0.5 *v/v/v*), S₂ DCM/methanol (95:5, *v/v*), S₃ DCM/EtOAc (9:1, *v/v*), S₄ DCM/MeOH (97.5:2.5 *v/v*), S₅ DCM/EtOAc (14:1 *v/v*). ¹H NMR and ¹³C NMR spectra were recorded using an FT-NMR 500 MHz spectrometer (Joel Ltd., Akishima, Tokyo, Japan). The chemical shifts (δ) are reported in ppm and were calculated concerning the frequency of the deuterium field stabilization signal. The coupling constant *J* is reported in Hertz. Signal multiplets are represented by the following abbreviations: s (singlet), brs (broad singlet), d (doublet), dd (doublet of doublets), dt (doublet of triplets), t (triplet), q (quintet), m (multiplet). Diastereoselectivity was characterized by ds (major/minor) according to ¹H NMR spectra [22]. UPLC separations were carried out according to the procedures described elsewhere [23].

Medium and supplements for *P. falciparum* culture and cell culture (RPMI 1640 Medium, Glutamine, Hepes Buffer, Fetal calf serum) were from EuroClone (Milan, Italy). AlbuMax and MCDD 131 medium were from Invitrogen (Milan, Italy). Unless stated otherwise, all reagents were from Sigma Italia (Milan, Italy).

3.2. Synthetic Procedures

3.2.1. General Method for Synthesis of the 1-Substituted-Tetrahydro- β -Carboline-3-Carboxylic Acids (1a–e)

According to the literature, a mixture of 0.5 N H₂SO₄ (2.5 mL) and H₂O (200 mL), D, L-tryptophan (2.04 g, 10 mmol), and appropriate aldehydes (30 mmol) was stirred at room temperature overnight and the synthesis products detected by TLC. The precipitate was filtered and washed well with H₂O and dried in a vacuum. The material was used without further purification for the following steps.

3.2.2. General Method for Synthesis of the 3-Carboxamide Derivatives of 1-Substituted-Tetrahydro- β -Carboline-3-Carboxylic Acids (**2–14**)

The appropriate 1-substituted-tetrahydro- β -carboline-3-carboxylic acid (**1a–e**) (1 equiv) suspensions in dichloromethane (DCM) with EDC (1.3 equiv), DMAP (0.5 equiv), HOBT (1.3 equiv), pyridine (0.05 equiv), and a relevant amine (1 equiv) were refluxed for 18 h. When the reactions were completed, the mixtures were extracted with CHCl_3 /isopropanol (3:1 *v/v*; 3×10 mL). The combined organic fractions were dried over Na_2SO_4 and evaporated under vacuum. The crude products were purified by crystallization in hexane or by column chromatography.

- *N*-cyclooctyl-2,3,4,9-tetrahydro-1*H*-pyrido[3,4-*b*]indole-3-carboxamide (**2**): (3*RS*)

Compound **2** was prepared using 2,3,4,9-tetrahydro-1*H*-pyrido[3,4-*b*]indole-3-carboxylic acid (**1a**) (0.25 mmol, 0.058 g) and EDC (0.325 mmol, 0.062 g), HOBT (0.325 mmol, 0.043 g), DMAP (0.125 mmol, 0.015 g), pyridine (0.025 mmol, 2 μL) and cyclooctanamine (0.25 mmol, 38 μL) in 8 mL DCM. The product was purified by column chromatography over silica gel and obtained as a crystallized oil with a yield of 40% ($R_f = 0.29$ (S_2)). LC/MS: $\text{C}_{20}\text{H}_{27}\text{N}_3\text{O}$ (98%) *m/z*: 326.22, found: 326.07. ^1H NMR (500 MHz, CDCl_3) δ 8.05 (br. s., 1H), 7.49 (d, $J = 8.0$ Hz, 1H), 7.32–7.28 (m, 1H), 7.19–7.13 (m, 1H), 7.12–7.08 (m, 1H), 7.04 (d, $J = 8.0$ Hz, 1H), 4.07–3.98 (m, 3H), 3.52 (dd, $J = 4.87$ Hz, 10.60 Hz, 1H), 3.23 (dd, $J = 4.6$ Hz, 15.5 Hz, 1H), 2.82–2.74 (m, 1H), 1.92–1.81 (m, 2H), 1.69 (d, $J = 8.6$ Hz, 2H), 1.61–1.51 (m, 8H). ^{13}C NMR (126 MHz, CDCl_3) δ 171.5, 136.1, 132.3, 127.4, 121.8, 119.6, 118.1, 110.9, 108.6, 57.5, 49.1, 43.0, 32.3, 27.3, 25.5, 24.8, 23.8.

- (1-methyl-2,3,4,9-tetrahydro-1*H*-pyrido[3,4-*b*]indol-3-yl)(piperidin-1-yl)methanone (**3**): (1*RS*,3*SR*)-**3**/(1*RS*,3*RS*)-**3**

Compound **3** was prepared using 1-methyl-2,3,4,9-tetrahydro-1*H*-pyrido[3,4-*b*]indole-3-carboxylic acid (**1b**) (0.25 mmol, 0.058 g) and EDC (0.325 mmol, 0.062 g), HOBT (0.325 mmol, 0.043 g), DMAP (0.125 mmol, 0.015 g), pyridine (0.025 mmol, 2 μL) and piperidine (0.25 mmol, 26 μL) in 8 mL DCM. The product was purified by column chromatography over silica gel and obtained as a yellowish solid with a yield of 72% ($R_f = 0.25$ (S_2)). LC/MS: $\text{C}_{18}\text{H}_{23}\text{N}_3\text{O}$ (95%) *m/z*: 298.18, found: 298.28. ds: (1*RS*,3*SR*)-**3**/(1*RS*,3*RS*)-**3** = 70:3. ^1H NMR (500 MHz, CDCl_3) δ 8.62–8.54 (m, 1H), 7.42 (d, $J = 7.5$ Hz, 1H), 7.31 (s, 1H), 7.10 (d, $J = 7.16$ Hz, 1H), 7.08–7.03 (m, 1H), 4.30–4.23 (m, 1H), 4.08–4.03 (m, 1H), 3.59 (t, $J = 5.3$ Hz, 1H), 3.48–3.43 (m, 1H), 2.88–2.77 (m, 2H), 2.15 (s, 3H), 1.69–1.48 (m, 8H) *NH* proton was not detected. ^{13}C NMR (126 MHz, CDCl_3) δ 171.1, 136.5, 135.9, 126.9, 121.6, 119.4, 117.7, 112.1, 111.0, 107.0, 53.4, 46.5, 42.9, 30.9, 25.4, 24.4, 20.0

- *N*-cyclohexyl-1-methyl-2,3,4,9-tetrahydro-1*H*-pyrido[3,4-*b*]indole-3-carboxamide (**4**): (1*RS*,3*SR*)-**4**/(1*RS*,3*RS*)-**4**

Compound **4** was prepared using 1-methyl-2,3,4,9-tetrahydro-1*H*-pyrido[3,4-*b*]indole-3-carboxylic acid (**1b**) (0.25 mmol, 0.058 g) and EDC (0.325 mmol, 0.062 g), HOBT (0.325 mmol, 0.043 g), DMAP (0.125 mmol, 0.015 g), pyridine (0.025 mmol, 2 μL) and cyclohexanamine (0.25 mmol, 28 μL) in 8 mL DCM. The product was purified by column chromatography over silica gel and obtained as a yellowish solid with a yield of 74% ($R_f = 0.11$ (S_2)). LC/MS: $\text{C}_{19}\text{H}_{25}\text{N}_3\text{O}$ (96%) *m/z*: 311.20, found 311.15. ds: (1*RS*,3*SR*)-**4**/(1*RS*,3*RS*)-**4** = 10:4. ^1H NMR (500 MHz, CDCl_3) δ 8.40 (s, 1H), 7.47 (d, $J = 8.0$ Hz, 1H), 7.31 (d, $J = 8.0$ Hz, 1H), 7.18–7.08 (m, 2H), 7.07–6.98 (m, 1H), 4.21–4.10 (m, 1H), 3.89–3.77 (m, 1H), 3.54 (dd, $J = 4.6$, 11.5 Hz, 1H), 3.28 (ddd, $J = 2.0$, 4.6, 15.8 Hz, 1H), 2.69 (ddd, $J = 2.9$ Hz, 11.3 Hz, 15.6 Hz, 1H), 2.01–1.90 (m, 2H), 1.78–1.69 (m, 2H), 1.63 (td, $J = 3.6$ Hz, 12.9 Hz, 1H), 1.49 (d, $J = 6.9$ Hz, 3H), 1.45–1.31 (m, 3H), 1.30–1.11 (m, 3H). ^{13}C NMR (126 MHz, CDCl_3) δ 172.1, 137.1, 136.2, 127.4, 121.8, 119.6, 118.3, 111.1, 108.4, 58.0, 49.5, 48.0, 33.2, 25.5, 20.4

- *N*-(cyclohexylmethyl)-1-methyl-2,3,4,9-tetrahydro-1*H*-pyrido[3,4-*b*]indole-3-carboxamide (**5**): (1*RS*,3*SR*)-**5**/(1*RS*,3*RS*)-**5**

Compound **5** was prepared using 1-methyl-2,3,4,9-tetrahydro-1*H*-pyrido[3,4-*b*]indole-3-carboxylic acid (**1b**) (0.25 mmol, 0.058 g) and EDC (0.325 mmol, 0.062 g), HOBT (0.325 mmol, 0.043 g), DMAP (0.125 mmol, 0.015 g), pyridine (0.025 mmol, 2 μL) and cyclohexylmethanamine (0.25 mmol, 32 μL) in 8 mL DCM. The product was purified by

column chromatography over silica gel and obtained as a yellowish solid with a yield of 72% ($R_f = 0.25$ (S_2)). LC/MS: $C_{20}H_{27}N_3O$ (95%) m/z : 326.22, found 326.05. ds: (1*RS*,3*SR*)-5/(1*RS*,3*RS*)-5 = 10:4. 1H NMR (500 MHz, $CDCl_3$) δ 8.05 (s, 1H), 7.49 (d, $J = 7.5$ Hz, 1H), 7.27 (s, 1H), 7.19–7.17 (m, 1H), 7.17–7.13 (m, 1H), 7.11–7.07 (m, 1H), 4.23–4.17 (m, 1H), 3.59 (dd, $J = 4.6$ Hz, 11.5 Hz, 1H), 3.33–3.27 (m, 1H), 3.22–3.11 (m, 2H), 2.71 (ddd, $J = 2.6$ Hz, 11.5 Hz, 15.8 Hz, 1H), 1.74 (dd, $J = 3.4$ Hz, 13.1 Hz, 5H), 1.51–1.46 (m, 3H), 1.29–1.12 (m, 4H), 1.01–0.91 (m, 2H) *NH* proton was not detected. ^{13}C NMR (126 MHz, $CDCl_3$) δ 172.9, 170.6, 137.0, 136.1, 127.4, 121.9, 119.1, 110.9, 108.7, 77.0, 58.1, 49.5, 45.5, 38.1, 31.0, 26.0, 20.4

- *N*-(Adamantan-1-yl)-1-ethyl-2,3,4,9-tetrahydro-1*H*-pyrido[3,4-*b*]indole-3-carboxamide (6): (1*RS*,3*SR*)-6/(1*RS*,3*RS*)-6

Compound 6 was prepared using 1-ethyl-2,3,4,9-tetrahydro-1*H*-pyrido[3,4-*b*]indole-3-carboxylic acid (1c) (0.25 mmol, 0.061 g) and EDC (0.325 mmol, 0.062 g), HOBT (0.325 mmol, 0.037 g), DMAP (0.125 mmol, 0.015 g), pyridine (0.025 mmol, 2 μ L) and adamantan-1-amine (0.25 mmol, 0.27 g) in 8 mL DCM. The product was purified by column chromatography over silica gel and obtained as a white solid with a yield of 60% ($R_f = 0.38$ (S_4)). LC/MS: $C_{24}H_{31}N_3O$ (96%) m/z : 378.25, found 378.30. ds: (1*RS*,3*SR*)-6/(1*RS*,3*RS*)-6 = 11 : 4.4. 1H NMR (500 MHz, $CDCl_3$) δ 8.62 (d, $J = 1.7$ Hz, 1H), 8.52 (s, 1H), 7.48–7.44 (m, 1H), 7.32–7.25 (m, 1H), 7.08–7.03 (m, 1H), 6.89 (s, 1H), 4.04 (d, $J = 5.2$ Hz, 1H), 3.44 (dd, $J = 4.6$ Hz, 10.9 Hz, 1H), 3.26 (ddd, $J = 1.7$ Hz, 4.4 Hz, 15.6 Hz, 1H), 2.67 (ddd, $J = 2.3$ Hz, 11.2 Hz, 15.8 Hz, 1H), 2.14–2.01 (m, 9H), 1.80 (ddd, $J = 4.6$ Hz, 7.4 Hz, 14.3 Hz, 1H), 1.74–1.62 (m, 7H), 1.03 (t, $J = 7.2$ Hz, 3H) *NH* indole was not detected. ^{13}C NMR (126 MHz, $CDCl_3$) δ 171.3, 135.0, 128.1, 120.9, 120.0, 119.0, 110.6, 107.1, 70.2, 56.3, 42.0, 36.1, 30.3, 27.2, 25.0, 11.1

- *N*-(3,3-dimethylbutyl)-1-octyl-2,3,4,9-tetrahydro-1*H*-pyrido[3,4-*b*]indole-3-carboxamide (7): (1*RS*,3*SR*)-7/(1*RS*,3*RS*)-7

Compound 7 was prepared using 1-octyl-2,3,4,9-tetrahydro-1*H*-pyrido[3,4-*b*]indole-3-carboxylic acid (1d) (0.5 mmol, 0.145 g) and EDC (0.65 mmol, 0.124 g), HOBT (0.65 mmol, 0.086 g), DMAP (0.25 mmol, 0.30 g), pyridine (0.025 mmol, 2 μ L) and 3,3-dimethylbutan-1-amine (0.5 mmol, 56 μ L) in 8 mL DCM. The product was purified by column chromatography over silica gel (DCM/EtOAc = 9:1) and obtained as a dark yellow oil with a yield of 15% ($R_f = 0.22$ (S_3)). LC/MS: $C_{26}H_{41}N_3O$ (96%) m/z : 412.32, found 412.28. ds: (1*RS*,3*SR*)-7/(1*RS*,3*RS*)-7 = 10:4.7. 1H NMR (500 MHz, $CDCl_3$) δ 7.85–7.70 (m, 1H), 7.52 (d, $J = 7.7$ Hz, 1H), 7.32 (dd, $J = 8.0$ Hz, 17.8 Hz, 1H), 7.19–7.14 (m, 1H), 7.17–7.08 (m, 1H), 7.05–7.00 (m, 1H), 4.14 (dd, $J = 2.0$ Hz, 4.9 Hz, 1H), 3.55 (dd, $J = 4.3$ Hz, 11.2 Hz, 1H), 3.40–3.30 (m, 3H), 2.70 (ddd, $J = 2.6$ Hz, 11.5 Hz, 15.5 Hz, 1H), 2.02–1.93 (m, 1H), 1.75 (q, $J = 7.5$ Hz, 1H), 1.67–1.43 (m, 4H), 1.39–1.25 (m, 8H), 1.00–0.95 (m, 9H), 0.90 (t, $J = 6.7$ Hz, 6H). ^{13}C NMR (126 MHz, $CDCl_3$) δ 135.9, 127.5, 121.9, 119.7, 118.4, 110.8, 109.5, 57.8, 53.8, 43.4, 35.9, 31.9, 29.5, 22.7, 14.2.

- 1-(4-chlorophenyl)-*N*-(3,3-dimethylbutyl)-2,3,4,9-tetrahydro-1*H*-pyrido[3,4-*b*]indole-3-carboxamide (8): (1*RS*,3*SR*)

Compound 8 was prepared using 1-(4-chlorophenyl)-2,3,4,9-tetrahydro-1*H*-pyrido[3,4-*b*]indole-3-carboxylic acid (1e) (0.25 mmol, 0.081 g) and EDC (0.325 mmol, 0.062 g), HOBT (0.325 mmol, 0.043 g), DMAP (0.125 mmol, 0.015 g), pyridine (0.1 mmol, 8 μ L) and 3,3-dimethylbutan-1-amine (0.25 mmol, 33 μ L) in 15 mL DCM. The product was purified by column chromatography over silica gel and obtained as an off-white solid with a yield of 22% ($R_f = 0.11$ (S_3)). LC/MS: $C_{24}H_{28}ClN_3O$ (97%) m/z : 410.20, found: 410.03. 1H NMR (500 MHz, $CDCl_3$) δ 7.82 (s, 1H), 7.57 (d, $J = 8.0$ Hz, 1H), 7.30–7.24 (m, 4H), 7.18 (dd, $J = 1.2$ Hz, 8.0 Hz, 1H), 7.16–7.11 (m, 3H), 6.80–6.74 (m, 1H), 5.21 (s, 1H), 3.53–3.47 (m, 1H), 3.29 (s, 1H), 3.27–3.15 (m, 1H), 2.90–2.82 (m, 1H), 1.44–1.37 (m, 2H), 1.25 (d, $J = 1.1$ Hz, 2H), 0.91 (s, 9H). ^{13}C NMR (126 MHz, $CDCl_3$) δ 172.4, 139.1, 136.3, 134.2, 129.7, 127.1, 122.4, 119.9, 118.6, 110.7, 110.1, 60.5, 58.2, 43.3, 36.0, 29.8, 24.6, 21.0, 14.3

- 1-(4-chlorophenyl)-*N*-(2,4,4-trimethylpentan-2-yl)-2,3,4,9-tetrahydro-1*H*-pyrido[3,4-*b*]indole-3-carboxamide (9): (1*RS*,3*SR*)

Compound 9 was prepared using 1-(4-chlorophenyl)-2,3,4,9-tetrahydro-1*H*-pyrido[3,4-*b*]indole-3-carboxylic acid (1e) (0.25 mmol, 0.081 g) and EDC (0.325 mmol,

0.062 g), HOBT (0.325 mmol, 0.043 g), DMAP (0.125 mmol, 0.015 g), pyridine (0.1 mmol, 8 μ L) and 7,7-dimethyloctan-1-amine (0.25 mmol, 38 μ L) in 15 mL DCM. The product was purified by column chromatography over silica gel (DCM/EtOAc = 14:1) and obtained as an off-white solid with a yield of 50% (R_f = 0.33 (S_5)). LC/MS: $C_{26}H_{32}ClN_3O$ (96%) m/z : 438.22 found 438.05. 1H NMR (500 MHz, $CDCl_3$) δ 7.58 (s, 1H), 7.55–7.52 (m, 1H), 7.38–7.30 (m, 2H), 7.28–7.21 (m, 3H), 7.18–7.09 (m, 2H), 6.84 (s, 1H), 5.14 (t, J = 2.3 Hz, 1H), 3.58 (dd, J = 4.3 Hz, 11.1 Hz, 1H), 3.38–3.28 (m, 1H), 2.80–2.70 (m, 1H), 1.74 (s, 2H), 1.67–1.60 (m, 1H), 1.43 (s, 6H), 1.00 (s, 9H). ^{13}C NMR (126 MHz, $CDCl_3$) δ 171.4, 139.4, 136.3, 134.0, 129.6, 127.2, 122.3, 119.2, 110.8, 58.2, 52.2, 26.1

- 1-(4-chlorophenyl)-*N*-((tetrahydrofuran-2-yl)methyl)-2,3,4,9-tetrahydro-1*H*-pyrido[3,4-*b*]indole-3-carboxamide (**10**): (1*RS*,3*SR*)

Compound **10** was prepared using 1-(4-chlorophenyl)-2,3,4,9-tetrahydro-1*H*-pyrido[3,4-*b*]indole-3-carboxylic acid (**1e**) (2.3 mmol, 0.76 g) and EDC (3.0 mmol, 0.58 g), HOBT (3.0 mmol, 0.4 g), DMAP (1.17 mmol, 0.143 g), pyridine (0.1 mmol, 8 μ L) and (tetrahydrofuran-2-yl)methanamine (2.3 mmol, 0.24 g) in 15 mL DCM. The product was purified by crystallization in hexane and a few drops acetone and obtained as an off-white solid with a yield of 35% (R_f = 0.09 (S_3)). LC/MS: $C_{23}H_{24}ClN_3O_2$ (95%) m/z : 410.16, found: 410.10. 1H NMR (500, $DMSO-d_6$) δ ppm: 10.75 (d, J = 3.0 Hz, 1H), 7.97–7.87 (m, 1H), 7.45–7.38 (m, 1H), 7.37–7.28 (m, 2H), 7.25–7.18 (m, 2H), 7.21 (t, J = 7.4 Hz, 1H), 7.01 (t, J = 6.7 Hz, 1H), 6.97–6.90 (m, 1H), 5.18 (br. s, 1H), 3.85–3.50 (m, 3H), 3.38–2.99 (m, 4H), 2.90 (dd, J = 4.6 Hz, J = 15.1 Hz, 1H), 2.77–2.56 (m, 1H), 1.85–1.64 (m, 3H), 1.54–1.29 (m, 1H). ^{13}C NMR (126 MHz, $DMSO-d_6$) δ ppm: 172.7, 142.0, 136.1, 131.6, 130.2, 128.0, 128.0, 126.7, 120.9, 118.4, 117.7, 111.1, 108.1, 108.1, 77.1, 77.0, 67.2, 67.2, 53.2, 42.5, 42.4, 28.5, 28.4, 25.2, 25.2

- *N*-((1,4-dioxan-2-yl)methyl)-1-(4-chlorophenyl)-2,3,4,9-tetrahydro-1*H*-pyrido[3,4-*b*]indole-3-carboxamide (**11**): (1*RS*,3*SR*)

Compound **11** was prepared using 1-(4-chlorophenyl)-2,3,4,9-tetrahydro-1*H*-pyrido[3,4-*b*]indole-3-carboxylic acid (**1e**) (2.3 mmol, 0.76 g) and EDC (3.0 mmol, 0.58 g), HOBT (3.0 mmol, 0.4 g), DMAP (1.17 mmol, 0.143 g), pyridine (0.1 mmol, 8 μ L) and (1,4-dioxan-2-yl)methanamine (2.3 mmol, 0.27 g) in 15 mL DCM. The product was purified by crystallization in hexane and obtained as a white solid with a yield of 15% (R_f = 0.07 (S_3)). LC/MS: $C_{23}H_{24}ClN_3O_3$ (98%) m/z : 426.15, found 426.04. 1H NMR (500, $DMSO-d_6$) δ ppm: 10.72 (s, 1H), 7.99–7.85 (m, 1H), 7.44–7.40 (m, 1H), 7.38–7.33 (m, 2H), 7.26–7.17 (m, 3H), 7.04–6.90 (m, 2H), 5.18 (br.s., 1H), 3.71–3.46 (m, 5H), 3.43–3.35 (m, 2H), 3.19–3.02 (m, 4H), 2.90 (dd, J = 15.5 Hz, 1H), 2.76–2.61 (m, 1H). ^{13}C NMR (126 MHz, $DMSO-d_6$) δ ppm: 172.9, 142.0, 136.1, 134.0, 131.7, 130.2, 128.1, 126.7, 121.0, 118.4, 117.7, 111.1, 108.0, 73.6, 73.6, 68.7, 65.9, 65.9, 53.2, 51.7, 25.0

- 1-(4-chlorophenyl)-*N*-(3-morpholinopropyl)-2,3,4,9-tetrahydro-1*H*-pyrido[3,4-*b*]indole-3-carboxamide (**12**): (1*RS*,3*SR*)-**12**/(1*RS*,3*RS*)-**12**

Compound **12** was prepared using 1-(4-chlorophenyl)-2,3,4,9-tetrahydro-1*H*-pyrido[3,4-*b*]indole-3-carboxylic acid (**1e**) (1.2 mmol, 0.39 g) and EDC (1.5 mmol, 0.30 g), HOBT (1.5 mmol, 0.20 g), DMAP (0.6 mmol, 0.07 g), pyridine (0.05 mmol, 4 μ L) and (1.2 mmol, 175 μ L) in 10 mL DCM. The obtained crude product was purified by column chromatography over silica gel (DCM/methanol = 95:5) and obtained as pink needlelike crystals with a yield of 45% (R_f = 0.1 (S_2)). LC/MS: $C_{25}H_{29}ClN_4O_2$ (96%) m/z : 453.20, found 453.04. ds: (1*RS*,3*SR*)-**12**/(1*RS*,*RS*)-**12** = 10:1.5. 1H NMR (500, $CDCl_3$) δ ppm: 8.00–7.89 (m, 1H), 7.70–7.58 (m, 2H), 7.39–7.34 (m, 3H), 7.30–7.19 (m, 4H), 5.34 (s, 1H), 3.68 (t, J = 4.0 Hz, 4H), 3.56 (dd, J = 10.5 Hz, 1H), 3.50–3.33 (m, 3H), 3.03–2.92 (m, 1H), 2.56–2.44 (m, 6H), 1.76 (quin, J = 6.5 Hz, 2H), *NH* proton was not detected. ^{13}C NMR (126 MHz, $CDCl_3$) δ ppm: 172.7, 139.9, 136.2, 133.9, 132.5, 129.9, 129.2, 128.7, 126.9, 122.3, 119.8, 118.5, 110.9, 110.4, 66.7, 66.7, 66.7, 57.3, 54.8, 53.8, 53.6, 52.4, 25.3, 25.0

- 1-(4-chlorophenyl)-*N*-cyclohexyl-2,3,4,9-tetrahydro-1*H*-pyrido[3,4-*b*]indole-3-carboxamide (**13**)

Compound **13** was prepared using 1-(4-chlorophenyl)-2,3,4,9-tetrahydro-1*H*-pyrido[3,4-*b*]indole-3-carboxylic acid (**1e**) (0.25 mmol, 0.081 g) and EDC (0.325 mmol,

0.062 g), HOBT (0.325 mmol, 0.043 g), DMAP (0.125 mmol, 0.015 g), pyridine (0.1 mmol, 8 μ L) and cyclohexanamine (0.25 mmol, 28 μ L) in 4 mL DCM. The obtained product (mixture of *cis* and *trans* isomers) was purified and diastereoisomers were separated by column chromatography over silica gel (R_f = 0.3 and R_f = 0.29 (S_5), overall yield 67%. LC/MS: $C_{24}H_{26}ClN_3O$ (96%) m/z : 408.94, found: 409.01.

- (1*RS*,3*SR*)-1-(4-chlorophenyl)-*N*-cyclohexyl-2,3,4,9-tetrahydro-1*H*-pyrido[3,4-*b*]indole-3-carboxamide (*trans*-13)

1H NMR (500 MHz, $CDCl_3$) δ 7.94 (s, 1H), 7.57 (d, J = 7.4 Hz, 1H), 7.32–7.28 (m, 3H), 7.20 (dt, J = 1.1 Hz, 7.4 Hz, 1H), 7.17–7.13 (m, 3H), 6.75 (d, J = 8.6 Hz, 1H), 5.19 (s, 1H), 3.78–3.70 (m, 1H), 3.52 (dd, J = 4.6 Hz, 9.7 Hz, 1H), 3.28 (dd, J = 4.9 Hz, 15.8 Hz, 1H), 2.88 (ddd, J = 1.7 Hz, 9.9 Hz, 15.9 Hz, 1H), 2.10–1.99 (br.s., 1H), 1.93–1.83 (m, 2H), 1.70 (tdd, J = 4.1 Hz, 8.6 Hz, 16.5 Hz, 2H), 1.62 (td, J = 3.7 Hz, 12.6 Hz, 1H), 1.43–1.30 (m, 2H), 1.25–1.08 (m, 3H). ^{13}C NMR (126 MHz, $CDCl_3$) δ 171.6, 139.8, 136.2, 133.8, 132.5, 129.9, 128.7, 127.0, 122.3, 119.7, 118.5, 110.9, 110.5, 54.7, 52.3, 47.7, 33.1, 32.9, 25.5, 24.8, 24.7

- (1*SR*,3*SR*)-1-(4-chlorophenyl)-*N*-cyclohexyl-2,3,4,9-tetrahydro-1*H*-pyrido[3,4-*b*]indole-3-carboxamide (*cis*-13)

1H NMR (500 MHz, $CDCl_3$) δ 7.58–7.52 (m, 2H), 7.37–7.33 (m, 2H), 7.26–7.24 (m, 2H), 7.23–7.20 (m, 1H), 7.17–7.09 (m, 2H), 6.74 (d, J = 8.6 Hz, 1H), 5.15 (t, J = 2.3 Hz, 1H), 3.84–3.74 (m, 1H), 3.66 (dd, J = 4.3 Hz, 11.1 Hz, 1H), 3.33 (ddd, J = 1.7 Hz, 4.4 Hz, 15.6 Hz, 1H), 2.82 (ddd, J = 2.3 Hz, 11.1 Hz, 15.8 Hz, 1H), 1.96–1.85 (m, 2H), 1.75–1.65 (m, 2H), 1.61 (td, J = 3.7 Hz, 13.1 Hz, 1H), 1.41–1.29 (m, 2H), 1.22–1.09 (m, 3H)

- 1-(4-chlorophenyl)-*N*-(cyclohexylmethyl)-2,3,4,9-tetrahydro-1*H*-pyrido[3,4-*b*]indole-3-carboxamide (14): (1*RS*,3*SR*)

Compound 14 was prepared using 1-(4-chlorophenyl)-2,3,4,9-tetrahydro-1*H*-pyrido[3,4-*b*]indole-3-carboxylic acid (1e) (0.25 mmol, 0.081 g) and EDC (0.325 mmol, 0.062 g), HOBT (0.325 mmol, 0.043 g), DMAP (0.125 mmol, 0.015 g), pyridine (0.1 mmol, 8 μ L) and cyclohexylmethanamine (0.25 mmol, 32 μ L) in 8 mL DCM. The product was purified by crystallization in hexane and a few drops of acetone to give a pale yellow solid with a yield of 25% (R_f = 0.09 (S_3)). LC/MS: $C_{25}H_{28}ClN_3O$ (96%) m/z : 422.19 found: 422.10. 1H NMR (500 MHz, $CDCl_3$) δ 7.76 (s, 1H), 7.57 (d, J = 8.0 Hz, 1H), 7.30–7.26 (m, 3H), 7.21–7.17 (m, 1H), 7.17–7.12 (m, 3H), 6.91 (t, J = 5.7 Hz, 1H), 5.23 (s, 1H), 3.56 (dd, J = 4.6 Hz, 9.7 Hz, 1H), 3.31 (dd, J = 5.1 Hz, 16.0 Hz, 1H), 3.16–3.09 (m, 1H), 3.02 (td, J = 6.4 Hz, 13.5 Hz, 1H), 2.89 (ddd, J = 1.4 Hz, 10.0 Hz, 16.0 Hz, 1H), 1.74–1.62 (m, 5H), 1.44 (ttd, J = 3.4 Hz, 7.3 Hz, 14.5 Hz, 1H), 1.29–1.07 (m, 4H), 0.95–0.85 (m, 2H). ^{13}C NMR (126 MHz, $CDCl_3$) δ 172.5, 139.3, 136.3, 134.6, 134.0, 130.0, 129.3, 127.2, 122.3, 119.9, 118.6, 111.1, 110.4, 58.4, 45.5, 38.0, 31.0, 26.5, 25.9

3.3. PKa and Log D Calculation

The decimal logarithm distribution coefficient (Log D) was calculated using the MarvinSketch software (v. 20.12.0, ChemAxon Ltd., Cambridge, MA, USA).

3.4. *P. falciparum* Cultures and Drug Susceptibility Assay

Plasmodium falciparum cultures were established according to the method of Trager and Jensen, with slight modifications [24]. The CQ-susceptible strain, D10, and the CQ-resistant strain, W2, were maintained in human type A-positive red blood cells at 5% hematocrit in RPMI 1640 medium with the addition of 1% AlbuMax, 0.01% hypoxanthine, 20 mM Hepes, and 2 mM glutamine. Cultures were maintained at 37 °C in a gas mixture consisting of 1% O_2 , 5% CO_2 , and 94% N_2 . Compounds were dissolved in DMSO and diluted with medium to achieve the required concentrations (final DMSO concentration <1%, which is non-toxic to the parasite). Drugs were introduced into 96-well flat-bottomed microplates and serial dilutions made. Asynchronous cultures with parasitaemia of 1–1.5% and 1% final hematocrit were aliquoted into the plates and incubated for 72 h at 37 °C. Parasite growth was determined spectrophotometrically (OD_{650}) by measuring the activity of parasite lactate dehydrogenase (pLDH), according to a modified version of the

method of Makler, in both control and drug-treated cultures [25]. The antimalarial activity is expressed as 50% inhibitory concentrations (IC_{50}); each IC_{50} value is the mean of at least three separate experiments performed in duplicate.

3.5. Cytotoxicity Assay on HMEC-1 Cell Line

The long-term human microvascular endothelial cell line (HMEC-1) was maintained in MCDB 131 medium supplemented with 10% fetal calf serum, 10 ng/mL of epidermal growth factor, 1 μ g/mL of hydrocortisone, 2 mM glutamine and 20 mM Hepes buffer. For the cytotoxicity assays, cells were treated with serial dilutions of test compounds and cell proliferation evaluated using the MTT assay. Plates were incubated for 72 h at 37 °C in 5% CO_2 , then 20 μ L of a 5 mg/mL solution of 3-(4,5-dimethylthiazol-2-yl)-2,5-diphenyltetrazolium bromide (MTT) in PBS was added for an additional 3 h at 37 °C. The plates were then centrifuged, the supernatants discarded, and the dark blue formazan crystals dissolved using 100 μ L of lysing buffer consisting of 20% (*w/v*) of a solution of SDS, 40% of *N,N* dimethylformamide in H_2O , at pH 4.7 adjusted with 80% acetic acid. The plates were then read on a microplate reader (Synergy 4 Bio-Tek Instruments, Thermo Fisher Scientific, Waltham, MA, USA) at a test wavelength of 550 nm and a reference wavelength of 650 nm. All the tests were performed in triplicate at least three times.

3.6. Determination of Hemolytic Activity

The study protocol was approved by the Bioethics Commission at the Lower Silesian Medical Chamber (1/PNHAB/2018, approval date 14 February 2018), and experiments were performed as previously described [26]. Compounds dissolved in DMSO were added in a volume corresponding to a final concentration of 10 μ M in the sample. Negative (erythrocytes in PBS buffer), positive (erythrocytes in distilled water), and DMSO controls were also prepared.

3.7. Molecular Modeling

Molecular modeling studies were performed to evaluate the possible mechanism of action of compound (1*S*,3*R*)-7. Crystal structures of five enzymes, whose activities are essential for the functioning of *P. falciparum*, were taken from the Protein Data Bank. These enzymes were: phosphoethanolamine methyltransferase (PMT—code 3UJ9), falcipain-2 (FP2—code 3BPF), falcipain-3 (FP3—code 3BPM), lactate dehydrogenase (LDH—code 1T26), and malate dehydrogenase (MDH—code 6R8G). All simulations were performed using the Small-Molecule Drug Discovery Suite (Schrödinger, Inc, New York, NY, USA). The crystal structure of each enzyme was refined using the Protein Preparation Wizard [27]: system pH was set at 7.4 ± 0.2 , all co-crystallized molecules (water molecules, other solvents using in the crystallization process), except a ligand (product/inhibitor/cofactor), were removed, hydrogen atoms were added, and the energy of the whole system was minimized using an OPLS3e force field. The structure of compound (1*S*,3*R*)-7 was optimized using the LigPrep tool (Schrödinger, Inc, New York, NY, USA). The proper protonation state at pH 7.4 was additionally verified using MarvinSketch software (ChemAxon, chemaxon.com accessed on 1st of April 2021, Cambridge, MA, USA). Induced-Fit Docking (IFD) was applied to dock compound (1*S*,3*R*)-7 to the selected enzyme crystal structures and its binding mode within each of the enzymes was evaluated [28]. For each crystal structure, the box centroid was set on the originally co-crystallized ligand: PMT—phosphocholine (product of the enzymatic reaction performed by PMT); FP2—epoxysuccinate (inhibitor); FP3—leupeptin (inhibitor); LDH—1,4-dihydropyridine adenine dinucleotide (NADH, cofactor); MDH—nicotinamide adenine dinucleotide (NAD, cofactor). No constraints were applied during IFD. Target-ligand complexes, obtained as an IFD output, were analyzed based on the observed molecular interactions. The observed binding modes of compound (1*S*,3*R*)-7 were compared with those captured for the ligands in the original crystal structures.

4. Conclusions

Malaria is still a major life-threatening infectious disease and, unfortunately, drug resistance to commonly used antimalarial drugs has become a serious problem. In this context, the search for new effective and selective agents active against this neglected parasite is obvious. Our studies led to the identification of a promising lead compound among a series of tetrahydro- β -carboline derivatives that were designed and tested. Compound **7** has the highest activity against *P. falciparum* and is without any toxicity at the tested dose of 10 μ M. Moreover, compound (1*S*,3*R*)-**7** has structural features enabling it to interact with enzymes essential for the functioning of *P. falciparum*, but a thorough explanation of its mechanism of action as well as the optimal delivery system are still required. Interestingly, the chemical structure of compound (1*S*,3*R*)-**7** also appears to aid in its stabilization within the protein crystal co-structures. Our results also provide a basis for further scaffold optimization, that could lead to the design, synthesis, and identification of additional compounds with improved antiparasitic potency.

Supplementary Materials: The following are available online at www.mdpi.com/article/10.3390/ijms222413569/s1.

Author Contributions: Conceptualization, A.J. and A.Z.; methodology, A.J., B.G., M.J., A.Z., S.P. and N.B.; software, M.J.; validation, A.J., B.G., M.J., A.Z., S.P. and N.B.; formal analysis, M.C.; investigation, A.J., B.G., M.J., S.P. and N.B.; resources, A.J., B.G., M.J., S.P., N.B. and A.Z.; data curation, A.J., B.G., M.J., A.Z., S.P. and N.B.; writing—original draft preparation, A.J., B.G., M.J. and A.Z.; writing—review and editing, A.J., S.P., N.B., D.T. and A.Z.; visualization, A.J., M.J., S.P., N.B. and A.Z.; supervision, A.J. and A.Z.; project administration, A.J. and N.B.; funding acquisition, A.J. and N.B. All authors have read and agreed to the published version of the manuscript.

Funding: The project is co-financed by the Polish National Agency for Academic Exchange (PPN/BIL/2018/2/00108) and the Italian Ministry of Foreign Affairs and International Cooperation “Executive Programme for Scientific and Technological Cooperation between the Italian Republic and the Republic of Poland” (PO19MO10). Publication of this article was financially supported by the Excellence Initiative—Research University (IDUB) program for the University of Wrocław.

Institutional Review Board Statement: Not applicable.

Informed Consent Statement: Not applicable.

Data Availability Statement: The data presented in this study are available in article or Supplementary Materials.

Conflicts of Interest: The authors declare no conflict of interest.

References

- World Malaria Report 2020. Available online: <https://www.who.int/teams/global-malaria-programme/reports/world-malaria-report-2020> (accessed on 11 October 2021).
- Available online: <https://www.who.int/news/item/06-10-2021-who-recommends-groundbreaking-malaria-vaccine-for-children-at-risk> (accessed on 23 October 2021).
- The “World Malaria Report 2019” at a Glance. Available online: <https://www.who.int/news-room/feature-stories/detail/world-malaria-report-2019> (accessed on 9 November 2020).
- Burrows, J.N.; Duparc, S.; Gutteridge, W.E.; Hooft Van Huijsduijnen, R.; Kaszubska, W.; Macintyre, F.; Mazzuri, S.; Möhrle, J.J.; Wells, T.N.C. New developments in anti-malarial target candidate and product profiles. *Malar. J.* **2017**, *16*, 26.
- Ariey, F.; Witkowski, B.; Amaratunga, C.; Beghain, J.; Langlois, A.C.; Khim, N.; Kim, S.; Duru, V.; Bouchier, C.; Ma, L.; et al. A molecular marker of artemisinin-resistant *Plasmodium falciparum* malaria. *Nature* **2014**, *505*, 50–55.
- Amaratunga, C.; Lim, P.; Suon, S.; Sreng, S.; Mao, S.; Sopha, C.; Sam, B.; Dek, D.; Try, V.; Amato, R.; et al. Dihydroartemisinin-piperaquine resistance in *Plasmodium falciparum* malaria in Cambodia: A multisite prospective cohort study. *Lancet Infect. Dis.* **2016**, *16*, 357–365.
- Leang, R.; Taylor, W.R.J.; Bouth, D.M.; Song, L.; Tarning, J.; Char, M.C.; Kim, S.; Witkowski, B.; Duru, V.; Domergue, A.; et al. Evidence of plasmodium falciparum multidrug resistance to artemisinin and piperaquine in Western Cambodia: Dihydroartemisinin-piperaquine open-label multicenter clinical assessment. *Antimicrob. Agents Chemother.* **2015**, *59*, 4719–4726.
- Bouwman, S.A.; Zoleko-Manego, R.; Renner, K.C.; Schmitt, E.K.; Mombo-Ngoma, G.; Grobusch, M.P. The early preclinical and clinical development of cipargamin (KAE609), a novel antimalarial compound. *Travel Med. Infect. Dis.* **2020**, *36*, 101765.

9. To Evaluate Efficacy, Safety, Tolerability and PK of Intravenous Cipargamin in Participants with Severe Plasmodium Falciparum Malaria-Full Text View-ClinicalTrials.gov. Available online: <https://clinicaltrials.gov/ct2/show/NCT04675931> (accessed on 27 September 2021).
10. Ghavami, M.; Merino, E.F.; Yao, Z.K.; Elahi, R.; Simpson, M.E.; Fernández-Murga, M.L.; Butler, J.H.; Casasanta, M.A.; Krai, P.M.; Totrov, M.M.; et al. Biological Studies and Target Engagement of the 2- C -Methyl- d -Erythritol 4-Phosphate Cytidyltransferase (IspD)-Targeting Antimalarial Agent (1 R,3 S)-MMV008138 and Analogs. *ACS Infect. Dis.* **2018**, *4*, 549–559.
11. Gorki, V.; Singh, R.; Walter, N.S.; Bagai, U.; Salunke, D.B. Synthesis and Evaluation of Antiplasmodial Efficacy of β -Carboline Derivatives against Murine Malaria. *ACS Omega* **2018**, *3*, 13200–13210.
12. Gellis, A.; Dumêtre, A.; Lanzada, G.; Hutter, S.; Ollivier, E.; Vanelle, P.; Azas, N. Preparation and antiprotozoal evaluation of promising β -carboline alkaloids. *Biomed. Pharmacother.* **2012**, *66*, 339–347.
13. Garg, A.; Lukk, T.; Kumar, V.; Choi, J.Y.; Augagneur, Y.; Voelker, D.R.; Nair, S.; Mamoun, C. Ben Structure, Function and Inhibition of the Phosphoethanolamine Methyltransferases of the Human Malaria Parasites Plasmodium vivax and Plasmodium knowlesi. *Sci. Rep.* **2015**, *5*, 1–13.
14. Makler, M.T.; Piper, R.C.; Milhous, W.K. Lactate Dehydrogenase and the Diagnosis of Malaria. *Parasitol. Today* **1998**, *14*, 376–377.
15. Chan, M.; Sim, T.S. Functional characterization of an alternative [lactate dehydrogenase-like] malate dehydrogenase in Plasmodium falciparum. *Parasitol. Res.* **2004**, *92*, 43–47.
16. Kerr, I.D.; Lee, J.H.; Pandey, K.C.; Harrison, A.; Sajid, M.; Rosenthal, P.J.; Brinen, L.S. Structures of Falcipain-2 and Falcipain-3 Bound to Small Molecule Inhibitors: Implications for Substrate Specificity. *J. Med. Chem.* **2009**, *52*, 852–857.
17. Song, H.J.; Liu, Y.X.; Liu, Y.X.; Huang, Y.Q.; Li, Y.Q.; Wang, Q.M. Design, synthesis, anti-TMV, fungicidal, and insecticidal activity evaluation of 1,2,3,4-tetrahydro- β -carboline-3-carboxylic acid derivatives based on virus inhibitors of plant sources. *Bioorganic Med. Chem. Lett.* **2014**, *24*, 5228–5233.
18. Eagon, S.; Hammill, J.T.; Bach, J.; Everson, N.; Sisley, T.A.; Walls, M.J.; Durham, J.; Pillai, D.R.; Falade, M.O.; Rice, A.L.; Kimball, J.J.; et al. Antimalarial activity of tetrahydro- β -carbolines targeting the ATP binding pocket of the Plasmodium falciparum heat shock 90 protein. *Bioorg. Med. Chem. Lett.* **2020**, *30*, 127502.
19. Shibeshi, M.A.; Kifle, Z.D.; Atnafie, S.A. Antimalarial Drug Resistance and Novel Targets for Antimalarial Drug Discovery. *Infect. Drug Resist.* **2020**, *13*, 4047–4060.
20. Imperatore, C.; Persico, M.; Senese, M.; Aiello, A.; Casertano, M.; Luciano, P.; Basilico, N.; Parapini, S.; Paladino, A.; Fattorusso, C.; et al. Exploring the antimalarial potential of the methoxy-thiazinoquinone scaffold: Identification of a new lead candidate. *Bioorg. Chem.* **2019**, *85*, 240–252.
21. Sonawane, D.P.; Persico, M.; Corbett, Y.; Chianese, G.; Di Dato, A.; Fattorusso, C.; Tagliatela-Scafati, O.; Taramelli, D.; Trombini, C.; Dhavale, D.D.; et al. New antimalarial 3-methoxy-1,2-dioxanes: Optimization of cellular pharmacokinetics and pharmacodynamics properties by incorporation of amino and N-heterocyclic moieties at C4. *RSC Adv.* **2015**, *5*, 72995–73010.
22. Ungemach, F.; Soerens, D.; Weber, R.; DiPierro, M.; Campos, O.; Mokry, P.; Cook, J.M.; Silverton, J. V. General Method for the Assignment of Stereochemistry of 1,3-Disubstituted 1,2,3,4-Tetrahydro- β -carbolines by Carbon-13 Spectroscopy. *J. Am. Chem. Soc.* **1980**, *102*, 6976–6984.
23. Jaromin, A.; Czopek, A.; Parapini, S.; Basilico, N.; Misiak, E.; Gubernator, J.; Zagórska, A. Synthesis and Antiplasmodial Activity of Novel Bioinspired Imidazolidinedione Derivatives. *Biomolecules* **2021**, *11*, 33.
24. Trager, W.; Jensen, J.B. Human malaria parasites in continuous culture. *Science* **1976**, *193*, 673–675.
25. Makler, M.T.; Hinrichs, D.J. Measurement of the lactate dehydrogenase activity of Plasmodium falciparum as an assessment of parasitemia. *Am. J. Trop. Med. Hyg.* **1993**, *48*, 205–210.
26. Jaromin, A.; Korycińska, M.; Piętka-Ottlik, M.; Musiał, W.; Peczyńska-Czoch, W.; Kaczmarek, Ł.; Kozubek, A. Membrane perturbations induced by new analogs of neocryptolepine. *Biol. Pharm. Bull.* **2012**, *35*, 1432–1439.
27. Sastry, G.M.; Adzhigirey, M.; Day, T.; Annabhimoju, R.; Sherman, W. Protein and ligand preparation: Parameters, protocols, and influence on virtual screening enrichments. *J. Comput. Aided. Mol. Des.* **2013**, *27*, 221–234.
28. Sherman, W.; Day, T.; Jacobson, M.P.; Friesner, R.A.; Farid, R. Novel procedure for modeling ligand/receptor induced fit effects. *J. Med. Chem.* **2006**, *49*, 534–553.